JOURNAL OF THE ROYAL SOCIETY Interface

Mapping protein electron transfer pathways with QM/MM methods

Victor Guallar and Frank Wallrapp

J. R. Soc. Interface 2008 **5**, 233-239
doi: 10.1098/rsif.2008.0061.focus

Interface focus

J. R. Soc. Interface (2008) **5**, S233–S239
doi:10.1098/rsif.2008.0061.focus
Published online 29 April 2008

Mapping protein electron transfer pathways with QM/MM methods

Victor Guallar* and Frank Wallrapp

Life Science Department, Barcelona Supercomputing Center, Jordi Girona, 29, 08034 Barcelona, Spain

Mixed quantum mechanics/molecular mechanics (QM/MM) methods offer a valuable computational tool for understanding the electron transfer pathway in protein–substrate interactions and protein–protein complexes. These hybrid methods are capable of solving the Schrödinger equation on a small subset of the protein, the quantum region, describing its electronic structure under the polarization effects of the remainder of the protein. By selectively turning on and off different residues in the quantum region, we are able to obtain the electron pathway for short- and large-range interactions. Here, we summarize recent studies involving the protein–substrate interaction in cytochrome P450 camphor, ascorbate peroxidase and cytochrome *c* peroxidase, and propose a novel approach for the long-range protein–protein electron transfer. The results on ascorbate peroxidase and cytochrome *c* peroxidase reveal the importance of the propionate groups in the electron transfer pathway. The long-range protein–protein electron transfer has been studied on the cytochrome *c* peroxidase–cytochrome *c* complex. The results indicate the importance of Phe82 and Cys81 on cytochrome *c*, and of Asn196, Ala194, Ala176 and His175 on cytochrome *c* peroxidase.

Keywords: quantum mechanics/molecular mechanics; compound I; haem; propionates; electron transfer

1. INTRODUCTION

Electron transfer is one of the simplest but crucial reactions in biochemistry present in almost all enzymatic cycles (Beratan *et al.* 1992; Langen *et al.* 1995). It might involve a relatively short pathway, for example from a substrate directly bound in the vicinity of the acceptor group, or a large pathway, for example across protein–protein complexes, where the donor and the acceptor might be considerably apart from each other. In any of these cases, obtaining direct information of the electron pathway is not a trivial task. Such atomic and electronic detailed information, however, is very valuable in terms of a better understanding of the enzymatic cycle, which might lead to more efficient protein inhibitor design.

The usual experimental procedure to determine the electron transfer pathway is by means of direct protein mutation. While this technique can probe the importance of some residues in the electron migration, it also has some disadvantages. First, performing the mutation of many residues is time and money consuming. Second, the mutation might bring some secondary effects, such as structural changes or significant perturbation of the electrostatics, which might mask the real cause for the loss of electron conductivity. Here, computational tools offer an alternative approach that might reduce the time and expenses of further experimental work to map the electron transfer pathway (Roitberg *et al.* 1998; Liang *et al.* 2004; Lin *et al.* 2005). They do not introduce any perturbation on the system and have the spatial and temporal resolution needed. They require, however, a fair resolution crystal structure to start with. With the actual rate of computer and quantum chemistry methodologies development, it is approaching the time when most experimental studies will initially perform a simulation.

Currently, there are various programs capable of obtaining an approximate electron transfer pathway. They are based on topological search algorithms finding the shortest pathways between the defined electron donor and acceptor (Kurnikov 2000), or on approximate, semi-empirical extended Hückel level of theory (Balabin & Onuchic 1996, 2000; Gehlen *et al.* 1996) for instance. The current increase in computational resources, together with the recent development of mixed quantum mechanics/molecular mechanics (QM/MM) algorithms, however, allow us to design more rigorous methodologies capable of tracking the electron delocalization (Skourtis & Beratan 1997; Gruschus & Kuki 1999; Improta *et al.* 2006; Migliore *et al.* 2006). QM/MM methods contain the elements to properly describe the potential energy surfaces relevant to biological and chemical processes (Mo & Gao 2000; Reuter *et al.* 2000; Vreven *et al.* 2003; Friesner & Guallar 2005; Senn & Thiel 2007). The reactive region of the active site can be studied with a robust *ab initio* QM methodology, employing a QM region of sufficient size to encompass any important electronic structure

*Author for correspondence (victor.guallar@bsc.es).

One contribution of 9 to a Theme Supplement 'Biomolecular simulation'.

Received 8 February 2008
Accepted 9 April 2008

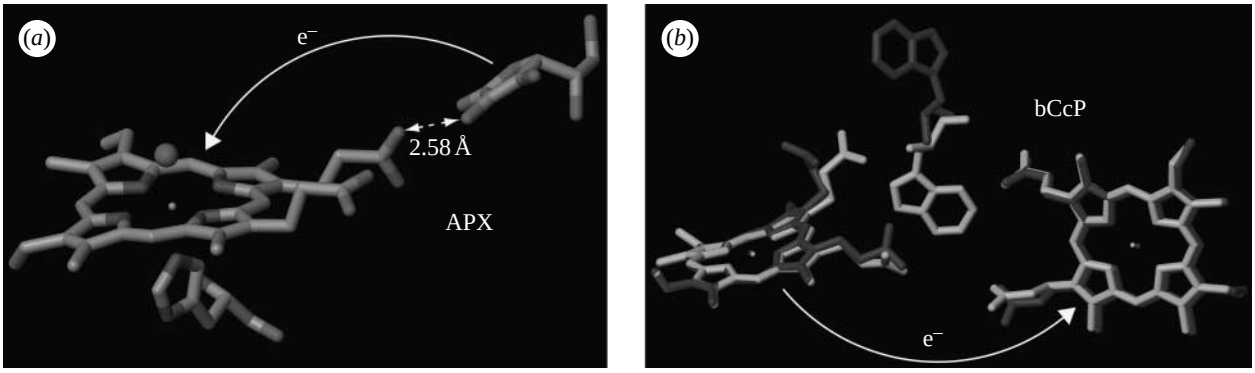

Figure 1. (*a*) Ascorbate arrangement in the ascorbate peroxidase crystal structure. The substrate is located in the hydrogen bond distance from the haem 7-propionate side chain. (*b*) Main changes in the active (light grey) and inactive (dark grey) crystal structures for the bacterial cytochrome *c* peroxidase.

effects. The remainder of the protein can be modelled at the cheaper MM theoretical level, providing the appropriate structural constraints, and the electrostatic and van der Waals non-bonding interactions with the core reactive region. Current computational resources, for example eight processors on an SGI Altix cluster, allow one to perform a wave-function analysis for a large quantum region, of the order of 400 atoms, in approximately 1–2 days.

In QM/MM methods, the Schrödinger equation is only solved for those atoms included in the quantum region (QM region). The MM or classical region is described by a set of 'solid' spheres with point charges. Electrons can only flow (or localize) between those atoms in the QM region. Thus, one can imagine multiple combinations of including/excluding residues in the QM region aiming to underline the pathway taken by the electron from the donor to the acceptor. Some approaches, currently under study in our laboratory, will be presented below.

Our interest in electron transfer pathway and spin delocalization started when studying the enzymatic cycle of cytochrome P450 camphor (Ortiz de Montellano 1995). We were particularly interested in compound I (Cpd I), an oxyferryl species known to be a major player in oxidative catalysis in cytochromes and peroxidases (Egawa *et al.* 1994; Wirstam *et al.* 1999; Jones & Dunford 2005). Cpd I is an iron(IV) oxyferryl species with two unpaired electrons in an iron–oxo moiety and a third unpaired electron localized in a porphyrin or protein radical. Owing to its high reactive nature, characterization of Cpd I has been particularly elusive (Jones & Dunford 2005). Besides the problems related to its short lifetime, the complexity of the system obscures the specific location of the radical. Computational modelling offers the possibility of studying the electron delocalization by means of solving the time-independent Schrödinger equation. Our studies pointed to an electron delocalization of the third unpaired electron in the propionate side chains of the porphyrin (Guallar *et al.* 2003; Guallar & Friesner 2004). These results generated much controversy among theoreticians and have been lately revised by several groups (Schoneboom *et al.* 2004; Altun *et al.* 2006, 2007; Guallar & Olsen 2006; Zheng *et al.* 2006; Zurek *et al.* 2006).

The observed delocalization of the spin density in the propionate side chains in Cpd I fitted well with several crystallographic structures. Figure 1*a* depicts the substrate arrangement in the ascorbate peroxidase crystal complex (APX), in direct contact with the haem propionates, substantially removed from the iron centre (Sharp *et al.* 2003). This protein, and in particular its Cpd I intermediate, uses electrons from the ascorbate to perform its peroxidase biochemistry. In figure 1*a*, we show a scheme of the haem Cpd I intermediate, indicating the metal iron centre and the oxo ligand (the iron–oxo moiety). Additional evidence of the importance of the propionates in APX comes from mutation studies (Barrows & Poulos 2005).

Remarkable crystallographic support for the active role of the propionates also comes from the bacterial di-haem cytochrome *c* peroxidase (bCcP) from *Pseudomonas nautica* 617. bCcP is one of the simplest prototypes for multicentre electron transfer proteins, containing a high-potential electron-transferring haem and a low-potential peroxidatic haem. The catalytic peroxidatic haem follows a hydrogen peroxide decomposition biochemistry. The enzyme activation event, observed crystallographically by Dias *et al.* (2004), is triggered by an essential calcium ion. Upon activation, there is a large rearrangement resulting in a direct link connecting the two haem centres through the propionates and Trp94, as shown in figure 1*b*.

In this paper, we summarize recent results for the analysis of the electron delocalization in P450cam, for the transfer pathway in APX and bCcP, and propose a novel approach for long-range interactions in protein–protein complexes.

2. MATERIAL AND METHODS

Enzymes having a large number of atoms and where it is not possible to solve the Schrödinger equation for the entire system require, for example, a multiscale approach combining quantum and classical mechanics. Mixed QM/MM approaches have recently been developed, which can join together QM and MM representations of different segments of a complex condensed phase system (Gao *et al.* 1998; Gao & Truhlar 2002; Friesner & Guallar 2005). The conjunction of these technologies contains the elements necessary to properly describe the potential energy surfaces relevant to enzymatic chemistry. Starting from a crystallographic structure (or some other atomic

model), the system is divided into a quantum and a classical region. In the quantum region, the time-independent Schrödinger equation is solved by means of a self-consistent approach using a basis set centred at the atomic centres. The outcome produces a wave function (molecular orbitals) from which several electronic properties are extracted. The classical region is described by a set of solid atoms with fixed charges and radii. These atoms are parametrized by a force field including bonding and non-bonding classical terms.

The models for P450cam, the substrate-bound APX and the di-haem bCcP systems were obtained from the 1DZ9, 1OAF and the 1RZ5 crystals, respectively. Preparation of the system included soaking the protein in a box of pre-equilibrated water molecules followed by 100 ps molecular dynamics at 300 K using periodic boundary conditions. The system was slowly heated and cooled in the first and last 10 ps. (More general details on the methods and system preparation have been published elsewhere (Friesner & Guallar 2005).) For the QM/MM minimizations, only a 10 Å layer of water molecules surrounding the proteins was kept. Geometry optimizations were carried out using unrestricted DFT with the B3LYP functional in combination with the 6-31G* (LACVP* effective core potential for the iron) basis set. In all geometry calculations, the last layer of oxygen atoms from the explicit water solvent was constrained. For all intermediates, we calculated the quartet and doublet spin states. All calculations were performed with the QSITE program (2001, QSITE, Schrödinger, Inc., Portland, Oregon).

We performed calculations with different quantum regions in the QM/MM system. This procedure allows us to track the electron delocalization. The results presented in §3 are based on spin-density and molecular orbital plots describing the radical content of the different intermediates. The spin plots are obtained from a grid projection of the difference in the alpha- and beta-spin orbitals from an unrestricted wave function. They represent the total amount (and localization) of spin density. A Mulliken population analysis has also been used to approximately quantify the amount of radical character in specific groups, such as the metal centre, the ascorbate substrate, etc.

3. RESULTS

3.1. Short electron transfer. Electron delocalization in compound I

Cpd I is an iron(IV) oxyferryl species with two unpaired electrons in an iron–oxo moiety and a third unpaired electron localized in a porphyrin or protein radical. The specific location of this third unpaired electron changes among different enzymes; small differences in the active site can introduce significant changes in the spin localization. We have presented mixed QM/MM results indicating the partial delocalization of the third unpaired electron into the haem propionates (Guallar *et al.* 2003; Guallar & Friesner 2004). Compound I can be envisioned as the product of an intramolecular single electron transfer reaction from the porphyrin to a putative Fe^{V} centre, resulting in a

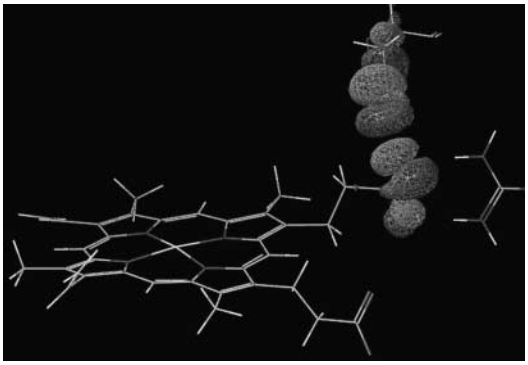

Figure 2. View of the molecular orbital for the proposed third unpaired electron in cytochrome P450 camphor.

Fe^{IV}–oxo moiety and a radicaloid porphyrin ligand. In this environment, our results indicated that the carboxylate is not electronegative enough to maintain fully occupied lone pair orbitals on its oxygen atoms, giving rise to a defect of electronic density on one of the propionates. Thus, the third unpaired electron partially delocalizes into the propionate groups. These results generated quite a controversy and produced several additional studies by us and other groups (Schoneboom *et al.* 2004; Altun *et al.* 2006, 2007; Guallar & Olsen 2006; Zheng *et al.* 2006; Zurek *et al.* 2006).

A close inspection of the propionates' vicinity in the P450cam crystal structure, 1DZ9, reveals a very interesting disposition of Asp297 (Schlichting *et al.* 2000). The oxygen–oxygen distance between the propionate and the carboxylic side chain of the aspartic residue is only approximately 2.3 Å. Such a short distance cannot be modelled with a hydrogen bond. The crystal resolution and beta factors, however, do not indicate a large error in the experimental distance. Interestingly, the distance is reproduced, with a remarkable agreement when the aspartic acid is deprotonated and treated, in the computational modelling, inside the quantum region. In such a model, where the haem group and the aspartic acid are both treated at the quantum level of theory, electrons can flow freely between these two moieties. The results indicate a one-electron transfer from the duet propionate–aspartic to the metal centre (Guallar & Olsen 2006). Thus, the third unpaired electron moves, respectively delocalizes, all the way to Asp297. Figure 2 shows a plot of this third unpaired electron. As a result of this electron transfer, the duet propionate–aspartic has a total net charge of only −1 electron units, which is nicely screened by the close arginine (also shown in figure 2), allowing for the close O–O distance observed experimentally. These controversial observations, independently confirmed by the group of Thiel (Altun *et al.* 2007), much depends on the protonation state of some specific residues (for example Asp297). Further experimental and theoretical studies will be necessary to assess the large delocalization of the third unpaired electron into Asp297. This delocalization, however, seems not to affect the hydroxylation process of camphor; the third unpaired electron is rapidly filled after the first hydrogen atom transfer from the camphor substrate (Altun *et al.* 2007).

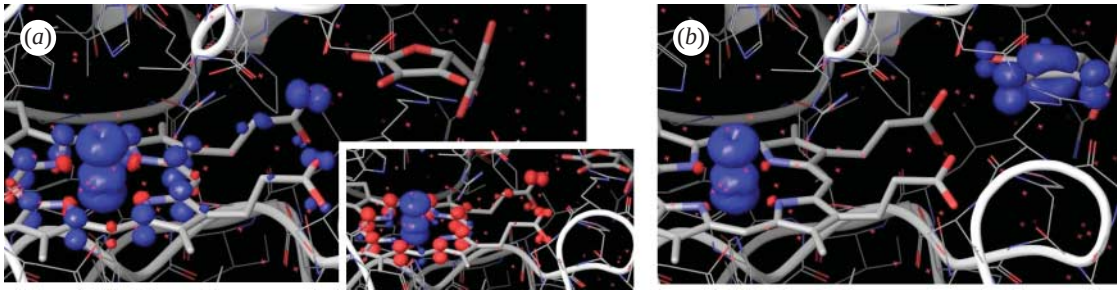

Figure 3. (*a*) Spin-density plot for the three unpaired electrons in APX when the ascorbate substrate is excluded from the quantum region. The main figure represents the quartet spin state and the inset shows the doublet spin state. (*b*) Spin density for the three unpaired electrons in APX when the ascorbate substrate is included in the quantum region (quartet spin state).

The results for P450cam indicate that Cpd I is capable of oxidizing residues in the vicinity of the haem group. This is obviously not a surprising result due to the known oxidation biochemistry of Cpd I and its numerous examples of forming covalent links to neighbour residues (Metcalfe *et al.* 2004; Pipirou *et al.* 2007). The fact that the electron might travel through the propionates is, however, a more controversial fact. These side chains have been observed classically as an electrostatic anchor for the haem group. This more modern view of the propionate side chains, however, does not seem so surprising when observing the arrangement of the ascorbate substrate in the ascorbate peroxidase complex (figures 1 and 3).

We have recently studied the three unpaired electrons in the ascorbate peroxidase Cpd I. The results are summarized in figure 3. In figure 3*b*, we observe the spin distribution when we include the haem group and the ascorbate substrate in the quantum region. As expected, Cpd I has oxidized the substrate and the third unpaired electron is located exclusively in the ascorbate. We should note here that for apo-APX, in the absence of the ascorbate substrate, the third unpaired electron is localized in the porphyrin cation radical (Patterson *et al.* 1995; Guallar & Olsen 2006). The result is very similar to that for P450cam, which oxidizes residue Asp297 (substrate for APX) in the vicinity of the propionates, as shown in figure 2. In the case of APX, however, the plots show the total spin density for all three unpaired electrons, having the first two located at the iron–oxo moiety (as seen in other Cpd I calculations; Ogliaro *et al.* 2000; Harris *et al.* 2001; Kamachi & Yoshizawa 2003; Zheng *et al.* 2006). In figure 3*b*, we show the results for the quartet spin state but analogous results are obtained for the doublet (Ogliaro *et al.* 2000; Kamachi & Yoshizawa 2003).

By employing mixed QM/MM methods, we can switch on and off the electronic description of different regions in the enzyme (namely the quantum and molecular mechanic region). Figure 3*a* displays the spin density for the same intermediate, having exactly the same structure as in figure 3*b* but with the ascorbate substrate excluded from the quantum region. Omitting the quantum description of the ascorbate eliminates the possibility of an electron transfer from this species to the iron metal centre. Thus, the QM region in figure 3*a* includes only the haem group (including the axial metal ligands). The first two unpaired electrons are located, as in figure 3*b*, in the iron–oxo moiety. The third unpaired electron clearly depicts a direct pathway connecting the iron centre to the substrate through the 7-propionate group. To point out the equivalence between the doublet and quartet spin states, we also show the doublet spin state in the inset in figure 3*a*.

Very similar results have also been obtained for the bacterial di-haem cytochrome *c* peroxidase. For this large di-haem system, we performed three calculations with three different quantum regions. The larger model included both the haem groups and the tryptophan bridging them in the quantum region. This model revealed, as expected, the one-electron transfer from the high-potential haem to the low-potential haem (sketch shown in figure 1). The second model excluded the high-potential haem from the QM region. The last model excluded both the high-potential haem and the bridging tryptophan residue. These last two models indicated the involvement of the tryptophan and the propionate groups in the electron transfer pathway connecting both metal centres.

3.2. Long electron transfer. Protein–protein interactions

The previous results indicate that a simple procedure, based on including/excluding residues to the quantum region in QM/MM simulations, can determine the electron pathway for short transfers. These results encouraged us to apply a similar scheme for long-range electron transfers. The novel methodology we have designed consists in the following procedure. We start by setting the parameters for both the donor and the acceptor matching the oxidized state. By doing so, the electron has already left the donor but has not yet arrived at the acceptor. This parametrization, consisting of a QM/MM calculation from which we extract the electrostatic potential fitted charges, is important since our procedure continues by placing both residues in the classical region. Thus, there is no electronic description of the donor and the acceptor in the quantum region. Instead, we focus on the 'transfer region' between them, the region that now contains the electron. We perform a first iteration including the entire transfer region in the QM subsystem and run a calculation where we add this electron to the system and specify a doublet spin state. Here, we are searching for the first receptor for the electron. Once we have located it, we proceed to the second iteration by turning the first identified residue into the classical description, excluding it from the

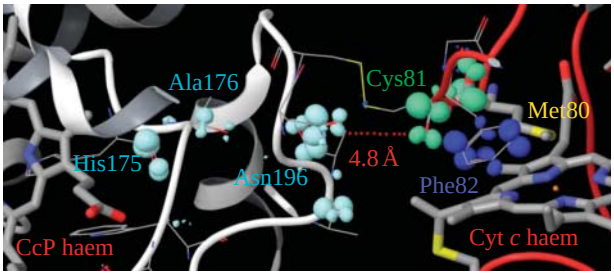

Figure 4. Electron transfer pathway for the CcP–Cyt *c* complex after three iterations of our procedure. Each iteration identifies the residue with the highest affinity for the electron and is shown in a different colour: blue, green and cyan.

quantum region. By excluding this residue, we do not allow an electronic description of it and thus the additional electron within the system needs to find another host. Hence, we look for a second electron acceptor in the transfer region. We iterate this procedure until we find a direct pathway connecting the donor and the acceptor. For very large transfer regions, the procedure could be applied to several subregions, of approximately 400 atoms (the present limit for current QM/MM methods), to cover the entire donor–acceptor distance. Thus, at this stage, the method consists in finding the residues with larger electron affinity in the transfer region, expecting that they will define an electron transfer pathway.

Figure 4 illustrates the preliminary results for the cytochrome *c* peroxidase–cytochrome *c* (CcP–Cyt *c*) complex. For this purpose, we have used the high-resolution crystal structure from the Poulos laboratory, 1SV6 (Guo *et al.* 2004). This structure presents a covalent link between the two proteins, which results in a high-resolution crystal. Additionally, this covalent structure closely mimics the physiological electron transfer complex (Guo *et al.* 2004). After placing the transfer region in the quantum region, adding one more electron and specifying a doublet spin state, the extra electron is localized in the side chain of Phe82 (a Cyt *c* residue), our first electron acceptor shown in blue in figure 4. This phenylalanine is located next to the donor haem, in direct contact with the methyonine (Met80), which acts as an axial ligand for the metal centre. We then proceeded by excluding this residue from the QM region. The second iteration placed the electron in the carbonyl group of Cys81 (also in the Cyt *c* protein), one of the cysteines involved in the covalent link of both proteins. This carbonyl group is only 4.8 Å apart from the CcP surface. This distance is shown with red dots in figure 4 and the second electron acceptor is shown in green in figure 4. The third iteration placed the electron in several residues in CcP. One of them is Asn196, in near contact with the carbonyl group of the previously mentioned Cys81, forming a close connection between the two proteins. In this third iteration, we find the residues connecting all the way to the acceptor haem in CcP. The pathway in this final stage of the electron transfer mainly involves the backbone carbonyl of Ala194, Ala176 and His175. This last histidine is one of the axial ligands for the metal centre in CcP and is also located next to the side chain of Trp191, which has been

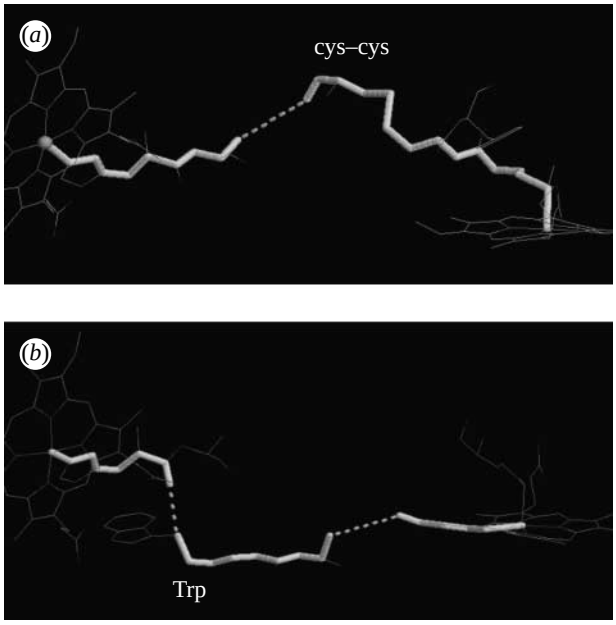

Figure 5. The two electron transfer pathways obtained with HARLEM. They correspond to the two crystal structures, (*a*) 1SV6 and (*b*) 2PCC, with CcP on the l.h.s. and Cyt *c* on the r.h.s.

proposed as the electron acceptor in CcP Cpd I (Pelletier & Kraut 1992; Guo *et al.* 2004). This last step is shown in cyan in figure 4. In summary, these preliminary results indicate an electron transfer pathway from haem in Cyt *c* through Phe82 (Cyt *c*), Cys81 (Cyt *c*), Asn196 (CcP) and His175 (CcP) into haem in CcP.

We should mention here that this procedure identifies the pathway including those residues with higher electron affinity in the transfer region. A shorter tunnelling pathway might differ substantially from it. Previous studies by Pelletier & Kraut (1992) and Beratan *et al.* (1992) have proposed a main pathway involving Ala194 (CcP) to Trp191 (CcP) that differs from ours. They used a method focusing on tunnelling contributions and, more importantly, a different initial structure without the sulphur–sulphur bridge (2PCC). Figure 5 shows the outcome of running HARLEM (Kurnikov 2000), a more approximate method aiming to characterize tunnelling pathways, on the two different crystal structures: 1SV6 (with the S–S bridge) and 2PCC. Clearly, two different pathways are obtained. Without the sulphur bridge, we recover the previous results of Pelletier & Kraut (1992) and Beratan *et al.* (1992). With the sulphur bridge, we obtain a pathway in very close agreement with the one obtained with our method. Thus, it seems that the sulphur bridge does affect considerably the electron transfer pathway (but not the enzymatic rate). In addition, our method seems to identify pathways close to the tunnelling regime. Obviously, we need to run more applications to corroborate this point.

Several other issues need to be addressed and we are currently working on them. First, we need to address the excess of electron delocalization, as shown in the third iteration. It is known that DFT methods tend to

delocalize the electron in the radical species (Harvey *et al.* 2006). Initial tests with an unrestricted Hartree–Fock wave function instead of a DFT one show good promise. Additional discussion might originate from the non-uniqueness of the electron transfer pathway. Several local parameters, for example protonation states, conformational changes, etc., might originate different pathways. Recent studies have suggested the important role of protein fluctuations on the electron transfer coupling mechanisms (Prytkova *et al.* 2007; Beratan & Balabin 2008). The method proposed, based on consecutive single-point calculations, is sufficiently fast to study different initial conditions and suggests alternative pathways. Current efforts in our laboratory are focusing on all-atom refinement of protein–protein docking and crystal structures, generating many conformations, which will undergo electron transfer characterization. Another interesting possible application is the study of alternative pathways after single mutations. At this stage, owing to the difference in quantum regions, it is not straightforward to obtain the electronic coupling between the different electron transfer states. Future work will focus on this problem as well as calculation of the electron transfer rates between the active sites (Prytkova *et al.* 2005).

In summary, we have shown that theoretical QM/MM methods are a valuable tool to characterize the electron transfer pathway for short and long distances. We propose a novel technique where we activate–deactivate different residues in the quantum region list in order to track the migration of the electron. Importantly, initial results for peroxidase systems indicate the active role of the haem propionate in conducting the electron, complementing the classical view of the propionate side chains as electrostatic anchors.

Computational resources were provided by the Barcelona Supercomputing Center. This work was supported by start-up funds from the Barcelona Supercomputing Center and through the Spanish Ministry of Education and Science through the project CTQ2006-10262/BQU.

REFERENCES

Altun, A., Guallar, V., Friesner, R. A., Shaik, S. & Thiel, W. 2006 The effect of heme environment on the hydrogen abstraction reaction of camphor in P450(cam) catalysis: a QM/MM study. *J. Am. Chem. Soc.* **128**, 3924–3925. (doi:10.1021/ja058196w)

Altun, A., Shaik, S. & Thiel, W. 2007 What is the active species of cytochrome p450 during camphor hydroxylation? QM/MM studies of different electronic states of compound I and of reduced and oxidized iron–oxo intermediates. *J. Am. Chem. Soc.* **129**, 8978–8987. (doi:10.1021/ja066847y)

Balabin, I. A. & Onuchic, J. N. 1996 Connection between simple models and quantum chemical models for electron-transfer tunneling matrix element calculations: a Dyson's equations-based approach. *J. Phys. Chem.* **100**, 11 573–11 580. (doi:10.1021/jp953568g)

Balabin, I. A. & Onuchic, J. N. 2000 Dynamically controlled protein tunneling paths in photosynthetic reaction centers. *Science* **290**, 114–117. (doi:10.1126/science.290.5489.114)

Barrows, T. P. & Poulos, T. L. 2005 Role of electrostatics and salt bridges in stabilizing the compound I radical in ascorbate peroxidase. *Biochemistry* **44**, 14 062–14 068. (doi:10.1021/bi0507128)

Beratan, D. N. & Balabin, I. A. 2008 Heme copper oxidases use tunneling pathways. *Proc. Natl Acad. Sci. USA* **105**, 403–404. (doi:10.1073/pnas.0711343105)

Beratan, D. N., Onuchic, J. N., Winkler, J. R. & Gray, H. B. 1992 Electron-tunneling pathways in proteins. *Science* **258**, 1740–1741. (doi:10.1126/science.1334572)

Dias, J., Alves, T., Bonifácio, C., Pereira, A., Trincão, J., Bourgeois, D., Moura, I. & Romão, M. 2004 Structural basis for the mechanism of Ca^{2+} activation of the di-heme cytochrome *c* peroxidase from *Pseudomonas nautica* 617. *Structure* **12**, 961–973. (doi:10.1016/j.str.2004.03.025)

Egawa, T., Shimada, H. & Ishimura, Y. 1994 Evidence for compound I formation in the reaction of cytochrome-P450cam with M-chloroperbenzoic acid. *Biochem. Biophys. Res. Commun.* **201**, 1464–1469. (doi:10.1006/bbrc.1994.1868)

Friesner, R. A. & Guallar, V. 2005 *Ab initio* quantum chemical and mixed quantum mechanics/molecular mechanics (QM/MM) methods for studying enzymatic catalysis. *Annu. Rev. Phys. Chem.* **56**, 389–427. (doi:10.1146/annurev.physchem.55.091602.094410)

Gao, J. & Truhlar, D. G. 2002 Quantum mechanical methods for enzyme kinetics. *Annu. Rev. Phys. Chem.* **53**, 467–505. (doi:10.1146/annurev.physchem.53.091301.150114)

Gao, J. L., Amara, P., Alhambra, C. & Field, M. J. 1998 A generalized hybrid orbital (GHO) method for the treatment of boundary atoms in combined QM/MM calculations. *J. Phys. Chem. A* **102**, 4714–4721. (doi:10.1021/jp9809890)

Gehlen, J. N., Daizadeh, I., Stuchebrukhov, A. A. & Marcus, R. A. 1996 Tunneling matrix element in Ru-modified blue copper proteins: pruning the protein in search of electron transfer pathways. *Inorganica Chim. Acta* **243**, 271–282. (doi:10.1016/0020-1693(95)04917-7)

Gruschus, J. M. & Kuki, A. 1999 Ellipsoidal delocalization of tunneling electrons in long-range electron transfer proteins. *J. Phys. Chem. B* **103**, 11 407–11 414. (doi:10.1021/jp9925280)

Guallar, V. & Friesner, R. A. 2004 Cytochrome P450CAM enzymatic catalysis cycle: a quantum mechanics/molecular mechanics study. *J. Am. Chem. Soc.* **126**, 8501–8508. (doi:10.1021/ja036123b)

Guallar, V. & Olsen, B. 2006 The role of the heme propionates in heme biochemistry. *J. Inorg. Biochem.* **100**, 755–760. (doi:10.1016/j.jinorgbio.2006.01.019)

Guallar, V., Baik, M.-H., Lippard, S. J. & Friesner, R. A. 2003 Peripheral heme substituents control the hydrogen-atom abstraction chemistry in cytochromes P450. *Proc. Natl Acad. Sci. USA* **100**, 6998–7002. (doi:10.1073/pnas.0732000100)

Guo, M., Bhaskar, B., Li, H., Barrows, T. P. & Poulos, T. L. 2004 Crystal structure and characterization of a cytochrome *c* peroxidase–cytochrome *c* site-specific cross-link. *Proc. Natl Acad. Sci. USA* **101**, 5940–5945. (doi:10.1073/pnas.0306708101)

Harris, D., Loew, G. & Waskell, L. 2001 Calculation of the electronic structure and spectra of model cytochrome P450 compound I. *J. Inorg. Biochem.* **83**, 309–318. (doi:10.1016/S0162-0134(00)00177-X)

Harvey, J. N., Bathelt, C. M. & Mulholland, A. J. 2006 QM/MM modeling of compound I active species in cytochrome P450, cytochrome *c* peroxidase, and ascorbate peroxidase. *J. Comput. Chem.* **27**, 1352–1362. (doi:10.1002/jcc.20446)

Improta, R., Barone, V. & Newton, M. D. 2006 A parameter-free quantum-mechanical approach for calculating electron-transfer rates for large systems in solution. *Chem. Phys. Chem.* **7**, 1211–1214.

Jones, P. & Dunford, H. B. 2005 The mechanism of compound I formation revisited. *J. Inorg. Biochem.* **99**, 2292–2298. (doi:10.1016/j.jinorgbio.2005.08.009)

Kamachi, T. & Yoshizawa, K. 2003 A theoretical study on the mechanism of camphor hydroxylation by compound I of cytochrome P450. *J. Am. Chem. Soc.* **125**, 4652–4661. (doi:10.1021/ja0208862)

Kurnikov, I. V. 2000 *HARLEM molecular modeling package*. Pittsburgh, PA: Department of Chemistry, University of Pittsburgh.

Langen, R., Chang, I. J., Germanas, J. P., Richards, J. H., Winkler, J. R. & Gray, H. B. 1995 Electron-tunneling in proteins—coupling through a beta-strand. *Science* **268**, 1733–1735. (doi:10.1126/science.7792598)

Liang, Z. X., Kurnikov, I. V., Nocek, J. M., Mauk, A. G., Beratan, D. N. & Hoffman, B. M. 2004 Dynamic docking and electron-transfer between cytochrome b5 and a suite of myoglobin surface-charge mutants. Introduction of a functional-docking algorithm for protein–protein complexes. *J. Am. Chem. Soc.* **126**, 2785–2798. (doi:10.1021/ja038163l)

Lin, J., Balabin, I. A. & Beratan, D. N. 2005 The nature of aqueous tunneling pathways between electron-transfer proteins. *Science* **310**, 1311–1313. (doi:10.1126/science.1118316)

Metcalfe, C. L., Ott, M., Patel, N., Singh, K., Mistry, S. C., Goff, H. M. & Raven, E. L. 2004 Autocatalytic formation of green heme: evidence for H_2O_2-dependent formation of a covalent methionine-heme linkage in ascorbate peroxidase. *J. Am. Chem. Soc.* **126**, 16 242–16 248. (doi:10.1021/ja048242c)

Migliore, A., Corni, S., Di Felice, R. & Molinari, E. 2006 First-principles density-functional theory calculations of electron-transfer rates in azurin dimers. *J. Chem. Phys.* **124**, 064 501–064 516. (doi:10.1063/1.2166233)

Mo, Y. R. & Gao, J. L. 2000 *Ab initio* QM/MM simulations with a molecular orbital-valence bond (MOVB) method: application to an S(N)2 reaction in water. *J. Comput. Chem.* **21**, 1458–1469. (doi:10.1002/1096-987X(200012)21:16<1458::AID-JCC4>3.0.CO;2-2)

Ogliaro, F., Harris, N., Cohen, S., Filatov, M., de Visser, S. P. & Shaik, S. 2000 A model "rebound" mechanism of hydroxylation by cytochrome P450: stepwise and effectively concerted pathways, and their reactivity patterns. *J. Am. Chem. Soc.* **122**, 8977–8989. (doi:10.1021/ja991878x)

Ortiz de Montellano, P. 1995 *Cytochrome P450: structure, mechanism and biochemistry*. New York, NY: Plenum.

Patterson, W. R., Poulos, T. L. & Goodin, D. B. 1995 Identification of a porphyrin pi cation radical in ascorbate peroxidase compound I. *Biochemistry* **34**, 4342–4345. (doi:10.1021/bi00013a024)

Pelletier, H. & Kraut, J. 1992 Crystal structure of a complex between electron transfer partners, cytochrome *c* peroxidase and cytochrome *c*. *Science* **258**, 1748–1755. (doi:10.1126/science.1334573)

Pipirou, Z., Bottrill, A. R., Metcalfe, C. M., Mistry, S. C., Badyal, S. K., Rawlings, B. J. & Raven, E. L. 2007 Autocatalytic formation of a covalent link between tryptophan 41 and the heme in ascorbate peroxidase. *Biochemistry* **46**, 2174–2180. (doi:10.1021/bi062274q)

Prytkova, T. R., Kurnikov, I. V. & Beratan, D. N. 2005 *Ab initio* based calculations of electron-transfer rates in metalloproteins. *J. Phys. Chem. B* **109**, 1618–1625. (doi:10.1021/jp0457491)

Prytkova, T. R., Kurnikov, I. V. & Beratan, D. N. 2007 Coupling coherence distinguishes structure sensitivity in protein electron transfer. *Science* **315**, 622–625. (doi:10.1126/science.1134862)

Reuter, N., Dejaegere, A., Maigret, B. & Karplus, M. 2000 Frontier bonds in QM/MM methods: a comparison of different approaches. *J. Phys. Chem. A* **104**, 1720–1735. (doi:10.1021/jp9924124)

Roitberg, A. E., Holden, M. J., Mayhew, M. P., Kurnikov, I. V., Beratan, D. N. & Vilker, V. L. 1998 Binding and electron transfer between putidaredoxin and cytochrome P450cam. Theory and experiments. *J. Am. Chem. Soc.* **120**, 8927–8932. (doi:10.1021/ja9739906)

Schlichting, I. *et al.* 2000 The catalytic pathway of cytochrome P450cam at atomic resolution. *Science* **287**, 1615–1622. (doi:10.1126/science.287.5458.1615)

Schoneboom, J. C., Cohen, S., Lin, H., Shaik, S. & Thiel, W. 2004 Quantum mechanical/molecular mechanical investigation of the mechanism of C–H hydroxylation of camphor by cytochrome P450(cam): theory supports a two-state rebound mechanism. *J. Am. Chem. Soc.* **126**, 4017–4034. (doi:10.1021/ja039847w)

Senn, H. M. & Thiel, W. 2007 QM/MM methods for biological systems. In *Atomistic approaches in modern biology: from quantum chemistry to molecular simulations*, vol. 268 (ed. M. Reiher). Topics in current chemistry, pp. 173–290. Berlin, Germany: Springer.

Sharp, K. H., Mewies, M., Moody, P. C. E. & Raven, E. L. 2003 Crystal structure of the ascorbate peroxidase–ascorbate complex. *Nat. Struct. Biol.* **10**, 303–307. (doi:10.1038/nsb913)

Skourtis, S. S. & Beratan, D. N. 1997 Electron transfer contact maps. *J. Phys. Chem. B* **101**, 1215–1234. (doi:10.1021/jp9619245)

Vreven, T., Morokuma, K., Farkas, O., Schlegel, H. B. & Frisch, M. J. 2003 Geometry optimization with QM/MM, ONIOM, and other combined methods. I. Microiterations and constraints. *J. Comput. Chem.* **24**, 760–769. (doi:10.1002/jcc.10156)

Wirstam, M., Blomberg, M. R. A. & Siegbahn, P. E. M. 1999 Reaction mechanism of compound I formation in heme peroxidases: a density functional theory study. *J. Am. Chem. Soc.* **121**, 10 178–10 185. (doi:10.1021/ja991997c)

Zheng, J., Wang, D., Thiel, W. & Shaik, S. 2006 QM/MM study of mechanisms for compound I formation in the catalytic cycle of cytochrome P450cam. *J. Am. Chem. Soc.* **128**, 13 204–13 215. (doi:10.1021/ja063439l)

Zurek, J., Foloppe, N., Harvey, J. N. & Mulholland, A. J. 2006 Mechanisms of reaction in cytochrome P450: hydroxylation of camphor in P450cam. *Org. Biomol. Chem.* **4**, 3931–3937. (doi:10.1039/b611653a)